

Available online at [www.sciencedirect.com](http://www.sciencedirect.com)**ScienceDirect**

Energy Procedia 55 (2014) 336 – 341

Energy

**Procedia**

4th International Conference on Silicon Photovoltaics, SiliconPV 2014

## Reliable interconnection of the front side grid fingers using silver-reduced conductive adhesives

Torsten Geipel\*, Md Zahidul Huq and Ulrich Eitner

*Fraunhofer Institute for Solar Energy Systems ISE, Heidenhofstrasse 2, 79110 Freiburg, Germany*

---

### Abstract

Electrically conductive adhesives as an alternative interconnection technology can potentially avoid the need for busbars on crystalline silicon solar cells. The adhesive is applied to the grid fingers and the ribbons for module integration can be directly attached to them. We analyze the interconnection related power losses by establishing an electrical model and validating the model with experimental I-V curve data. The maximum error is 7 % for one-cell-minimodules. In the following, we select silver-reduced adhesives and tin-coated ribbons to build minimodules and perform environmental chamber tests. The interconnection related cell-to-module losses are higher by 0.5 % compared to standard soldering on busbars. The minimodules with silver-reduced glues and tin-coated ribbons are stable in 1000 h damp heat and degrade by a maximum of 3 % after 200 thermal cycles. Only the highly Ag-filled acrylate failed the thermal cycling test.

© 2014 Published by Elsevier Ltd. This is an open access article under the CC BY-NC-ND license

(<http://creativecommons.org/licenses/by-nc-nd/3.0/>).

Peer-review under responsibility of the scientific committee of the SiliconPV 2014 conference

*Keywords:* photovoltaic module; module integration; electrically conductive adhesives; reliability; grid fingers; electrical loss

---

### 1. Introduction

Electrically conductive adhesives (ECA) is a lead-free, low thermo-mechanical stress, flexible and reliable alternative interconnection technology [1]. It is especially attractive for novel high-efficiency crystalline silicon solar cells like heterojunction or back-contact solar cells [2, 3]. It has previously been shown that the interconnection of the front side grid fingers without the necessity of busbars is a promising and reliable concept for

---

\* Corresponding author. Tel.: +49-761-45885023; fax: +49-761-45889193.

*E-mail address:* [torsten.geipel@ise.fraunhofer.de](mailto:torsten.geipel@ise.fraunhofer.de)

saving material costs [4] or for the enabling of new cell and metallization technologies like plated metallization or contacting transparent conductive oxides [5] which are difficult or impossible to solder.

The goals of our investigation are, first, to analyze the electrical losses associated with this approach by providing and validating a power loss model, second, to build and test minimodules for reliability with silver-reduced ECAs and silver-free ribbons. Silver-reduced glues are chosen due to their important role in the endeavour of overall cost reduction.

### Nomenclature

ECA	electrically conductive adhesive
$\Delta P_{Rs}$	power loss caused by the interconnection in the solar module (W)
$P_{l,contact}$	power loss caused at the contact areas of finger, adhesive and ribbon (W)
$P_{l,ribbon}$	power loss caused by the current flowing through the ribbon material (W)
$P_{l,gap}$	power loss caused in the gaps between adjacent cells (W)
$P_{l,sc}$	power loss in the string interconnection (W)
$I_{mpp,cell}$	current at the maximum power point at cell level (A)
$I_{ribbon,exit}$	exit current in one ribbon (A)
$I_{finger}$	current collected from one grid finger (A)
$R_{s,cell}$	series resistance of the solar cell ( $\Omega$ )
$R_{s,module}$	series resistance of the module ( $\Omega$ )
$m$	number of cells in the module
$s$	number of strings in the module
$c$	number of cells in the string
$n$	number of busbars
$k$	number of grid fingers
$j$	iteration variable
$r_{ribbonf}$	effective resistivity of the parallel connection of ribbon and ECA-layer on the front side ( $\Omega/m$ )
$r_{ribbonb}$	effective resistivity of the parallel connection of ribbon and metallization on the back side ( $\Omega/m$ )
$r_{gap}$	effective resistivity of the ribbon in the cell gap ( $\Omega/m$ )
$r_{sc}$	effective resistivity of the string interconnector ( $\Omega/m$ )
$\rho_{c,f}$	specific contact resistance of the contacted area on the front side ( $\Omega m^2$ )
$\rho_{c,b}$	specific contact resistance of the contacted area on back side ( $\Omega m^2$ )
$l_f$	length of the contacted area on the front side (m)
$l_b$	length of the contacted area on the back side (m)
$l_{sc}$	length of the string interconnector (m)
$l_g$	length of the cell gap (m)
$w_f$	width of the contacted area on the front side (m)
$w_b$	width of the contacted area on the back side (m)
$w_{finger}$	finger width (m)
$x$	position in the ribbon (m)

## 2. Modeling

Series resistance power losses due to the interconnection in the module ( $\Delta P_{Rs}$ ) are caused by the current of the cell matrix flowing through the interconnection components, which are:

- the contact areas from cell metallization through the interconnection material (solder or ECA) and the ribbon surface ( $P_{l,contact}$ )
- the ribbons attached to the cell ( $P_{l,ribbon}$ )

- the gaps between adjacent cells ( $P_{l,gap}$ )
- the string interconnectors ( $P_{l,sc}$ )

The sum of the individual loss components give the overall series resistance power loss in the solar module

$$\Delta P_{Rs} = P_{l,contact} + P_{l,ribbon} + P_{l,gap} + P_{l,sc} \quad (1)$$

Using the basic principle and approach described in [6-8] the individual loss components for an m-cell-module are given in equations (3)–(5). The table at the beginning of the paper defines the input parameters for the model.

The loss due to the contact resistance of the interconnection is given by

$$P_{l,contact} = m \left( kn(I_{finger})^2 \frac{\rho_{c,f}}{w_{finger} w_f} + n(I_{ribbonexit})^2 \frac{\rho_{c,b}}{l_b w_b} \right) \quad (2)$$

The loss caused by the lateral current flow in the ribbon is expressed with

$$P_{l,ribbon} = m \left( n \sum_{j=1}^k (j I_{finger})^2 r_{ribbonf} \frac{l_f}{k} + n \int_0^{l_b} \left( \frac{I_{ribbonexit}}{l_b} x \right)^2 r_{ribbonb} dx \right) \quad (3)$$

It must be noted that the specific metallization of the solar cell contributes to the lateral current flow out of the cell especially on the back side. For the case of continuous busbars, this contribution is included within the effective quantity  $r_{ribbon,b}$  as a parallel connection of effective metallization resistivity (busbar and full-area Aluminium) and ribbon resistivity. The same principle is used for the front side, such that  $r_{ribbonf}$  is modeled as a parallel connection of the effective ribbon resistivity, adhesive resistivity and, if existent, the busbar resistivity.

Usually the cells are made up of strings that are all serially connected. In this case the losses in the cell gaps are described with

$$P_{l,gap} = (c+1) \cdot s \cdot n (I_{ribbonexit})^2 r_{gap} \cdot l_g \quad (4)$$

The loss in the string interconnection depends on the exact geometry of the module and position of the cells and outgoing leads. We simplify for the case of a three busbar cell in a miniodule, such that  $m = 1$ ,  $m_{string} = 1$  and  $n = 3$  to validate the model later. Then, the loss in the string connection is approximately

$$P_{l,sc} = 2(I_{ribbonexit})^2 r_{sc} l_{sc} \quad (5)$$

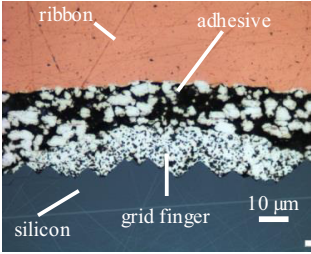
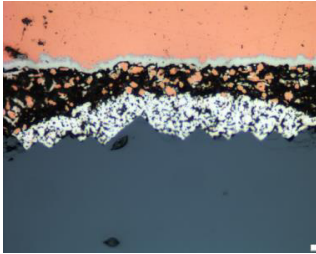
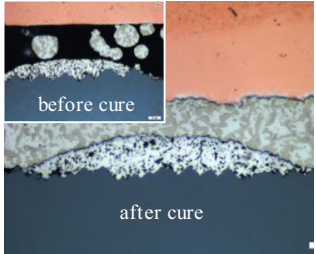
The input parameters like contact resistivities and effective resistivities of ribbon materials were determined experimentally by the transfer length method. The volume resistivities of the adhesives were taken from the data sheets.

### 3. Materials and methods

To validate the calculation model and to gather data about the reliability of the concept, one-cell-minimodules were produced. Mono-crystalline cells with screen printed continuous busbars on both sides are used. The interconnections on the grid fingers are implemented by glueing as close as possible to the busbars without touching them. The advantage is that no special equipment is needed for the I-V measurements at cell level such that an evaluation of the cell-to-module ratio is possible. A disadvantage is that the existing busbar may influence the outcome of the reliability test because it creates a short between the grid fingers. Any local degradation of the glued interconnection on grid fingers may be compensated by it.

Information about the conductive adhesives that are used for the experiments are presented in Table I. Approximately 15 mg glue per track is consumed.

Table I. Overview of the conductive adhesives used for experimentation

	a) silver-filled acrylate	b) silver and copper-filled epoxy	c) solder-filled epoxy
cross section			
composition	acrylate resin 75 – 85 w% silver 1 – 10 μm spheres	epoxy resin blend of silver and copper 1 – 3 μm flakes	epoxy resin low melting point solder particles
curing conditions	30 s at 150 °C	15 min at 150 °C	curing in two steps 1) bond formation at 150 °C in 10 s 2) epoxy cure at 140 °C in 20 min
peel strength	1.0 N/mm	0.4 N/mm	1.3 N/mm
contact resistance	0.18 mΩcm <sup>2</sup>	0.11 mΩcm <sup>2</sup>	0.12 mΩcm <sup>2</sup>

We use Sn-coated ribbons (2.0 mm × 0.15 mm, coating: 20 μm) for the glued interconnections and 1 μm Ag-coated ribbons with the same dimensions for the climate chamber reference modules. Soldered on busbar modules and soldering of the rear side, which was done for all samples, is made with SnPbAg-coated ribbons of the same dimensions.

The interconnection power loss  $\Delta P_{Rs}$  is calculated from the I-V measurements of cells and minimodules with

$$\Delta P_{Rs} = (R_{s,module} - R_{s,cell}) \cdot I_{mpp,cell}^2 \quad (6)$$

$R_{s,module}$  and  $R_{s,cell}$  are the series resistances obtained with the method in [9] at cell and module level respectively. Any optical changes from cell to module are excluded from our investigation, such that only  $I_{mpp,cell}$  is taken into account in this equation.

## 4. Results and discussion

### 4.1. Resin bleed and curing

The solder-filled epoxy must be cured in two steps. The first step is illustrated in fig. 1. A section of the solar cell is depicted where the solder-filled epoxy is dispensed on the grid fingers and the cell is placed on a heating plate with 150 °C. The series of images from (a) to (g) shows the first cure phase in a time of approximately 10 s.

It can be seen in (c) that the epoxy resin starts to »bleed out« onto the wafer surface. This is due to capillary action on the pyramid-like texturization of the silicon wafer [1, 3]. When the temperature reaches the melting point of the solder in (e), the particles start to melt and accumulate on the grid fingers. This is due to the fact that only the silver fingers are a solderable material.

This behaviour implies that the glue self-aligns on the grid fingers and is anisotropic such that the current flows only vertically towards the ribbon. The adhesive cannot contribute to the lateral current flow to the outgoing leads.

In a second curing step, the epoxy, which is to encapsulate the solder bonds in a rigid polymer matrix, is cured for 20 min at ~140 °C. The reduced temperature avoids remelting or de-soldering of the bonds.

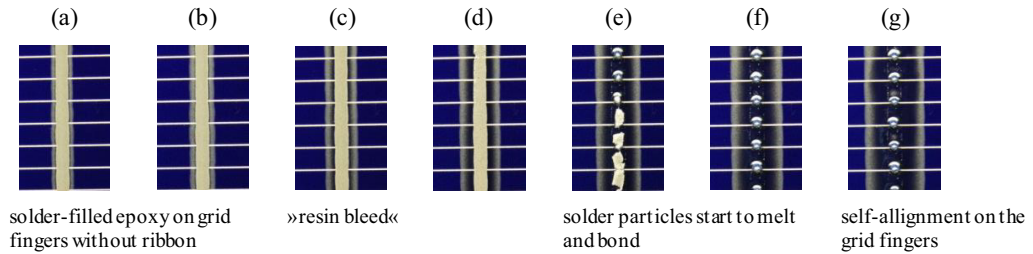


Fig. 1. First curing phase of the solder-filled epoxy at 150 °C.

4.2. Power losses of the interconnection

The results of the calculation of the additional power loss are shown in fig. 1b. In fig. 1a the comparison with soldering on busbar is given. The latter leads to an overall electrical loss of 3.2 % for a 60-cell-module with 240 Wp. The loss due to the contact resistance only accounts 1 % for the overall electrical loss.

The power loss of glueing directly on grid fingers is 3.7 %. As can be seen in the pie chart, the share of the contact resistance loss has increased to 11 % due to the reduction in available contact area. The contact resistance becomes a critical parameter for the total electrical loss in the module.

The results of the experimental assessment can be seen as full circles in fig. 3 together with the calculated values as open rectangles. The error bars at the experimental values denote the uncertainty among different specimen whereas the error bars at the calculated values represent a variation of the contact resistivity of  $\pm 0.02 \text{ m}\Omega\text{cm}^2$  to show the strong outcome of the simulation on a variation of the contact resistance.

The experimental results confirm the calculated values with a largest determined error of 7 %. The reasons for the deviation are the inaccuracy in contact resistance measurements and the compromises and flaws in module making.

The highly silver-filled acrylate shows the highest losses with 4.0 %. This is due to the high contact resistance of the adhesive. The Ag-Cu-filled epoxy has only a loss of 3.5 % due to the bulk ECA that contributes to the lateral current flow in the ribbon. The solder-filled epoxy shows 3.7 % power loss. It is higher due to its anisotropic conduction properties.

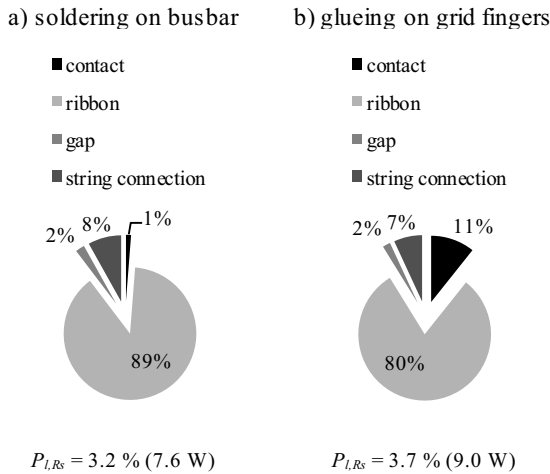


Fig. 2. Share of the total power loss of interconnection among the different loss components in the 60-cell-module.

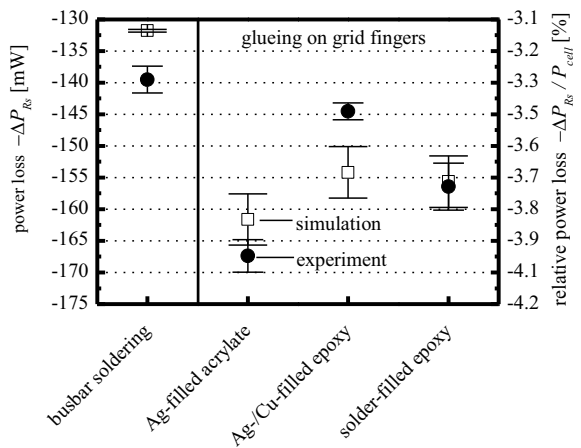


Fig. 3. Closed circles: Power loss of the interconnection of one-cell-minimodules. Open rectangles: Simulated data of the power loss.

### 4.3. Reliability

It can be seen in fig. 4 that the modules – regardless of the glue and ribbon used – show no significant degradation in 1000 h damp heat (DH 1000). The critical test is thermal cycling for 200 cycles (TC 200) because less contact area is existent with glueing on the grid fingers. The modules made of Ag-Cu-filled epoxy and solder-filled epoxy degrade by 2–3 % which is still within the limit specified by IEC 61215.

The Ag-filled acrylate in combination with the silver-coated ribbons fail TC 200 with a degradation of 46 %. It is assumed that resin bleed could be a reason for this effect. If the resin is drained onto the silicon surface too few resin will remain to secure the cohesion of the layer which becomes prone to cracking during thermal cycling.

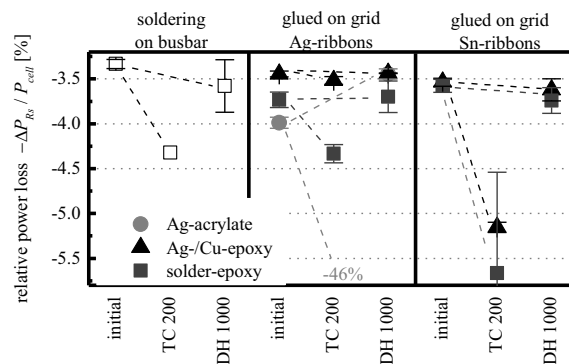


Fig. 4. Reliability data of the minimodules. Uncertainty of  $P_{cell} \sim 1.6\%$ , for  $R_s \sim 0.9\%$ .

## 5. Conclusion

We investigated the power loss of glueing on grid fingers by simulation and experiment. An additional power loss of approximately 0.5 % is to be expected depending on the contact resistance of the glue. We validated the model with a maximum error of 7 %. One-cell-minimodules with silver-reduced glues and silver-free ribbons were subjected to climatic chamber tests. No degradation in damp heat 1000 and a maximum of 3 % degradation in thermal cycling 200 is seen. The silver-filled acrylate failed the thermal cycling test possibly due to resin bleed.

## References

- [1] Beier B, Mau S, Metz A, Hezel R. Electrical conductive adhesives: A novel reliable method for interconnecting crystalline silicon solar cells. 17th EUPVSEC 2001:812-815.
- [2] Lamers M, Tjengdrawira C, Koppes M, Bennett I, Bende E, Visser T, Kossen E, Brockholz B, Mewe A, Romijn I. 17.9% Metal-wrap-through mc-Si cells resulting in module efficiency of 17.0%. Prog Photovoltaics 2012;20:62–73.
- [3] Scherff MLD, Schwertheim S, Yue M, Mueller T, Fahmer WR. 10 x 10 cm<sup>2</sup> HIT solar cells contacted with lead-free electrical conductive adhesives to solar cell interconnectors. 4th IEEE WCPEC 2006:1384-1387.
- [4] Schneider A, Hameya R, Aulehlaa S, Lemp E, Koch S. Progress in interconnection of busbar-less solar cells by means of conductive gluing. Energy Procedia 2013;38:387-394.
- [5] Schwertheim S, Scherff M, Mueller T, Fahmer WR, Neitzert HC. Lead-free electrical conductive adhesives for solar cell interconnectors. 33rd IEEE PVSC 2008:1-6.
- [6] Caballero LJ, Sanchez-Friera P, Lalaguna B, Alonso J, Vazquez MA. Series resistance modelling of industrial screen-printed monocrystalline silicon solar cells and modules including the effect of spot soldering. 4th IEEE WCPEC 2006:1388-1391.
- [7] Sánchez-Friera P, Roperio F, Lalaguna B, Caballero LJ, Alonso J. Power losses in crystalline silicon PV modules due to cell interconnection. 23rd EUPVSEC 2008:2701-2704.
- [8] Haedrich I, Eitner U, Hendrichs M-S, Spribille A, Wiese M, Wirth H. Unified methodology for determining CTM ratios: Systematic prediction of module power. this conference 2014.
- [9] Aberle AG, Wenham SR, Green MA. A new method for accurate measurement of the lumped series resistance of solar cells. 23rd IEEE PVSC 1993:133-139.